Article

Cell Reports

p53 Maintains Genomic Stability by Preventing Interference between Transcription and Replication

Graphical Abstract

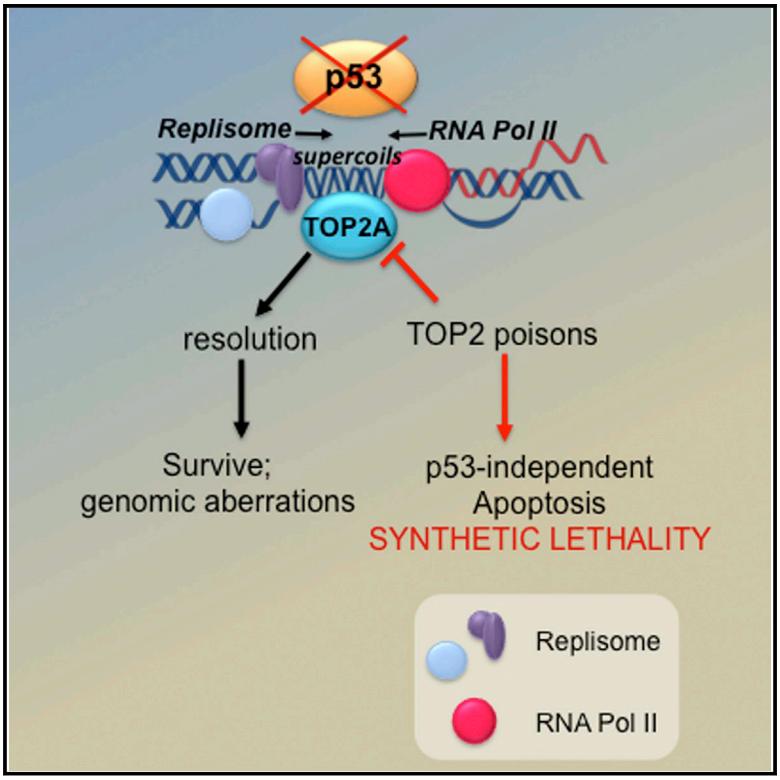

Authors

Constance Qiao Xin Yeo, Irina Alexander, Zhaoru Lin, ..., Vishal Pendharkar, Vincent H.B. Ho, Chit Fang Cheok

Correspondence

cfcheok@jrl.a-star.edu.sg

In Brief

Yeo et al. demonstrate that p53 maintains genomic stability during replication by preventing the interference between replication and transcription. Transcription inhibition restores fork progression and attenuates the sensitivity to Topo II inhibitors in p53-deficient cells, providing compelling evidence that transcription causes chronic replication stress in the absence of functional p53.

Highlights

- p53 loss causes increased topological conflict between transcription and replication
- p53 loss impairs normal replication fork progression
- Topological conflict and TOP2A recruitment are reversed by transcription inhibition
- Transcription inhibition also restores fork progression in p53-deficient cells

Yeo et al., 2016, Cell Reports *15*, 132–146
April 5, 2016
http://dx.doi.org/10.1016/j.celrep.2016.03.011

OPEN ACCESS
CellPress

Cell Reports
Article

p53 Maintains Genomic Stability by Preventing Interference between Transcription and Replication

Constance Qiao Xin Yeo,[1] Irina Alexander,[1,2] Zhaoru Lin,[1] Shuhui Lim,[1] Obed Akwasi Aning,[1] Ramesh Kumar,[1,2] Kanda Sangthongpitag,[4] Vishal Pendharkar,[4] Vincent H.B. Ho,[3] and Chit Fang Cheok[1,2,5,6,*]
[1]IFOM-p53Lab Joint Research Laboratory, Agency for Science, Technology and Research, Singapore 138648, Singapore
[2]IFOM, FIRC Institute of Molecular Oncology, 20139 Milan, Italy
[3]Molecular Engineering Laboratory, Agency for Science, Technology and Research, Singapore 138673, Singapore
[4]Experimental Therapeutics Center, Agency for Science, Technology and Research, Singapore 138669, Singapore
[5]Department of Biochemistry, Yong Loo Lin School of Medicine, National University of Singapore 117597, Singapore
[6]Lee Kong Chian School of Medicine, Nanyang Technological University, Singapore 308232, Singapore
*Correspondence: cfcheok@jrl.a-star.edu.sg
http://dx.doi.org/10.1016/j.celrep.2016.03.011

SUMMARY

p53 tumor suppressor maintains genomic stability, typically acting through cell-cycle arrest, senescence, and apoptosis. We discovered a function of p53 in preventing conflicts between transcription and replication, independent of its canonical roles. p53 deficiency sensitizes cells to Topoisomerase (Topo) II inhibitors, resulting in DNA damage arising spontaneously during replication. Topoisomerase IIα (TOP2A)-DNA complexes preferentially accumulate in isogenic p53 mutant or knockout cells, reflecting an increased recruitment of TOP2A to regulate DNA topology. We propose that p53 acts to prevent DNA topological stress originating from transcription during the S phase and, therefore, promotes normal replication fork progression. Consequently, replication fork progression is impaired in the absence of p53, which is reversed by transcription inhibition. Pharmacologic inhibition of transcription also attenuates DNA damage and decreases Topo-II-DNA complexes, restoring cell viability in p53-deficient cells. Together, our results demonstrate a function of p53 that may underlie its role in tumor suppression.

INTRODUCTION

Recent advances in our understanding of the mechanisms protecting the integrity of human genome have led to the realization that dysregulation of genome maintenance in cancer may leave tumor cells vulnerable to chemotherapeutic approaches exploiting genomic instability (Curtin, 2012; Lord and Ashworth, 2012). Oncogenes and/or loss of tumor suppressor protein function drive tumorigenesis by deregulating cell-cycle checkpoints, DNA repair, and apoptotic pathways. This leads to cell proliferation that is achieved at the expense of replication stress, causing DNA damage (Bartkova et al., 2005; Gorgoulis et al., 2005).

Replication stress is a crucial driver of genomic instability. Unrepaired DNA lesions, secondary DNA structures, and encounters with the transcription machinery may block the timely progression of the replisome. This causes the stalling and collapse of replication forks, leading to double-strand breaks (DSBs) and recombinogenic DNA structures, driving deleterious genome rearrangements. Analysis of early human precancerous lesions reveals hallmarks of activated DNA damage signaling, leading to a model whereby oncogene-induced hyperproliferation results in replication stress, increased DNA DSBs, and p53 induction, which poses a protective barrier against tumorigenesis (Halazonetis et al., 2008; Murga et al., 2011). It is thought that oncogenes cause increased origin firing that ultimately results in the overall spatial and temporal deregulation of DNA replication (Bester et al., 2011; Di Micco et al., 2006; Dominguez-Sola et al., 2007).

An important downstream consequence of these alterations in DNA replication is the potential for clashes with other processes occurring on the DNA strand, particularly transcription, resulting in replication fork collapse and DNA breaks. As a case in point, cyclin E overexpression has recently been shown to specifically increase transcription and replication interference, and the effects are ameliorated by inhibiting transcription (Jones et al., 2013). Therefore, proper coordination of replication and transcription is required during the S phase to avoid the risk of DNA damage. However, the key molecular players in these processes remain largely unidentified.

Although the p53 pathway is clearly central for genome maintenance, how it protects replicating DNA is not well understood. p53 has a myriad of functions aimed at both protecting the cell from genotoxic insult (pro-survival) and protecting the tissue and organism from neoplasm (pro-apoptosis) (Cheok et al., 2011; Lowe et al., 1993; Vousden and Prives, 2009). p53 imposes a senescence program or mediates cell-cycle arrest following DNA damage and replication stress to allow the repair of damaged DNA or to prevent further proliferation of damaged cells (Bunz et al., 1999; Jackson et al., 2012; Taylor et al., 1999). As a consequence, loss of p53, in conjunction with ATR suppression, results in a deleterious gene interaction due to the combined loss of G1 and S-G2 checkpoints (Nghiem et al., 2001; Reaper et al., 2011). Therefore, p53 deficiency, due to loss of a G1 checkpoint, leads to promiscuous S-phase entry that confers increased genomic instability and cell lethality

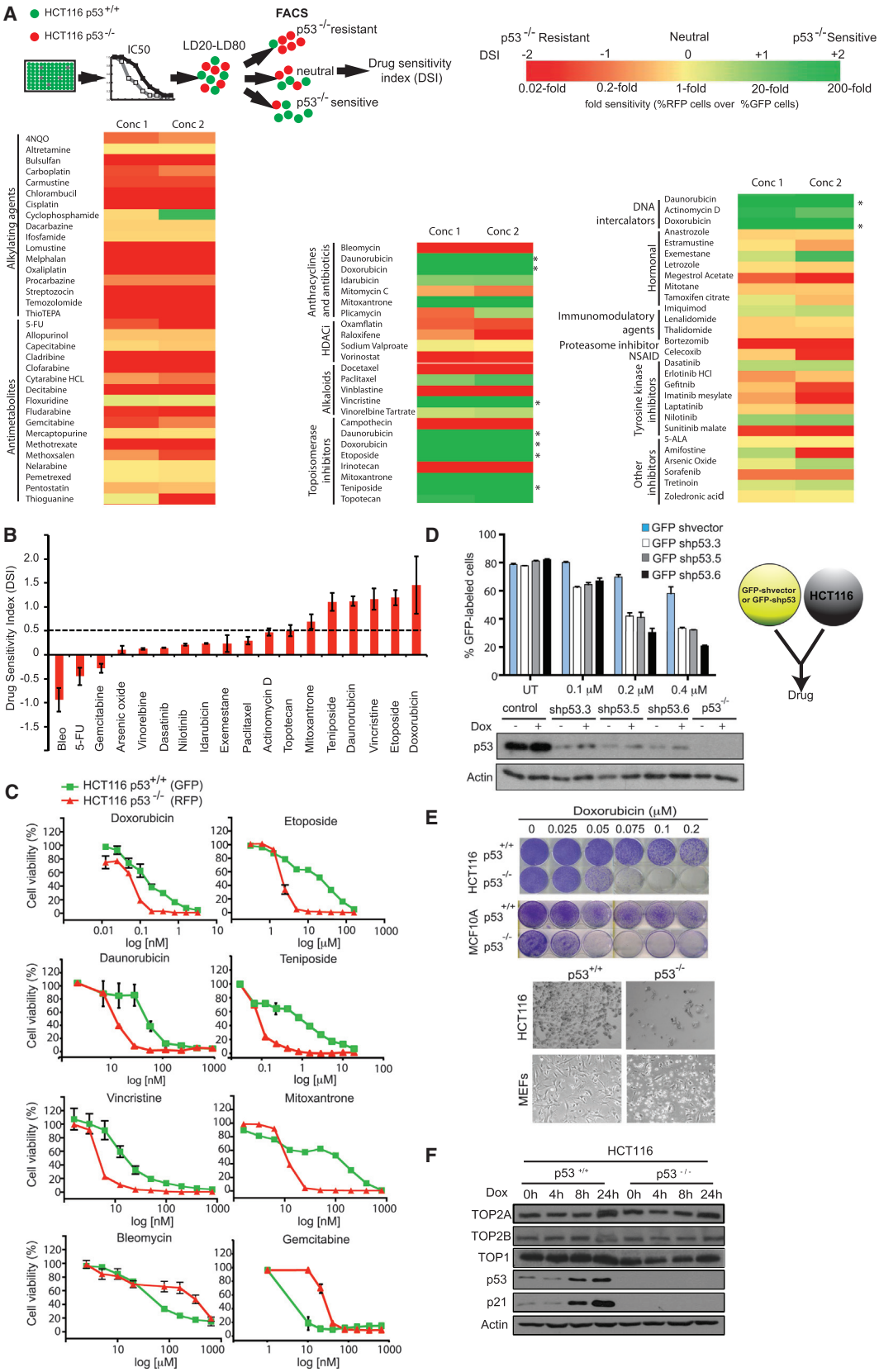

(legend on next page)

when ATR is suppressed (Murga et al., 2009; Schoppy et al., 2012; Toledo et al., 2011). In addition, loss of the G2 checkpoint maintenance in p53-deficient cells also sensitizes them to various forms of DNA damage (Bunz et al., 1998). However, it is uncertain whether p53 could play a more direct role during the S phase in ensuring replication integrity, which is independent of its canonical roles in cell-cycle checkpoint arrest.

Here, we show that the loss of wild-type p53 sensitizes cells toward topoisomerase (Topo) II poisons and results in increased DNA damage and replication defects that are reversed by transcription inhibition. We proposed that increased transcription-replication collisions, occurring in the absence of p53, generate elevated DNA torsional stress, which engages Topo II for resolution. We highlight an important role of p53, distinct from its canonical roles in cell-cycle checkpoint control, in maintaining genomic integrity and replication fidelity by preventing DNA topological conflicts between transcription and replication.

RESULTS

Unbiased Screen Reveals that p53-Deficient Cells Are Selectively Sensitive to Topo Inhibitors

p53 mutations are conventionally associated with resistance to chemotherapy due to loss of pro-apoptotic pathways (Oren and Rotter, 2010), but p53 deficiency has conversely been reported to increase sensitivity to doxorubicin (Dox) (Bunz et al., 1999), although the mechanism remains unclear. To delineate the mechanism explaining the paradoxical increase in sensitivity to Dox in p53-deficient cells, we performed an unbiased screen on a pair of isogenic HCT116 colon carcinoma cell lines differing only in p53 status (HCT116 $p53^{+/+}$ and HCT116 $p53^{-/-}$) (Bunz et al., 1998), using a panel of 83 FDA (Food and Drug Administration)-approved drugs, for drugs behaving similarly to Dox and thus identify common lesions that may sensitize p53-deficient cells (Table S1).

We established a robust and quantitative cytometry-based assay (differential fluorescence labeling of cells; DiFLC), to compare the relative viability of cocultured fluorescently labeled cells, the HCT116 $p53^{+/+}$ (GFP) and $p53^{-/-}$ (red fluorescent protein; RFP) cell lines, grown and treated under a single drug treatment condition. Cocultures of HCT116 $p53^{+/+}$ (GFP) and HCT116 $p53^{-/-}$ (RFP) cells were screened using drug concentrations (lethal dose [LD]20–LD80) that would ensure effective cell killing (Table S2) and avoid unspecific side effects. The Drug Sensitivity Index (DSI) (see Experimental Procedures) was determined from relative percentages of each cell type 5 days post-drug-recovery (Figure 1A). A positive DSI indicates that $p53^{-/-}$ cells were more sensitive to the drug, reflected in an increased GFP:RFP cell ratio, while a negative DSI indicates that $p53^{-/-}$ cells show decreased drug sensitivity.

p53 deficiency enhanced sensitivity to Topo-targeting compounds (Figures 1B and S1), resulting in high DSI values of >0.5. These included Dox, its derivative daunorubicin (Dau), etoposide (Etop, orVP-16), teniposide (Teni, or VM-26), and mitoxantrone (Figures 1B and S1), suggesting that Dox mainly acts on Topo and not via DNA intercalation and reactive oxygen species (Frederick et al., 1990; Kurz et al., 2004). As expected, p53 absence caused resistance to DNA-cytotoxic drugs, including DNA crosslinkers, DSB-inducing agents, and microtubule poisons, as previously reported (Bunz et al., 1999; Lowe et al., 1993), further demonstrating that the increased sensitivity of $p53^{-/-}$ cells does not apply to all DNA-damaging drugs.

Treatment with Topo II inhibitors markedly decreased colony survival and viability of HCT116 $p53^{-/-}$ cells compared to HCT116 $p53^{+/+}$ cells (Figures 1C and S1). Over 90% of cells surviving the highest concentration of Dox (0.2 μM) were $p53^{+/+}$ (GFP) cells (Figures S2A–S2C). p53 knockdown using different short hairpin (shRNA) constructs also resulted in a selective depletion of cells in a DiFLc assay (Figures 1D and S2D). This also resulted in a predominant G2/M arrest, similar to drug-treated HCT116 $p53^{-/-}$ cells (Figure S2E). In the human mammary epithelial MCF10A cell line, isogenic $p53^{-/-}$ cells were markedly more sensitive to Dox compared to wild-type cells (Figure 1E). Mouse embryonic fibroblasts (MEFs) harboring a genetic knockout of p53 gene were also greatly sensitized to Dox (Figure 1E), confirming that p53 loss specifically sensitizes cells of different genetic backgrounds, origins, and species to toxicity from Topo II inhibitors in vitro.

Lethal Phenotype Induced by Topo II Inhibitors Require TOP2A but Not TOP2B

Both HCT116 $p53^{+/+}$ and $p53^{-/-}$ cells expressed comparable amounts of all Topo I (TOP1), Topo IIα (TOP2A), and Topo IIβ (TOP2B) proteins, even with Dox treatment (Figure 1F). Thus, the increased sensitivity to Topo poisons of $p53^{-/-}$ cells cannot be simply explained by differential expression of Topo targets.

TOP2A and TOP2B are known targets of Topo poisons in cancer treatment (Burgess et al., 2008), but only TOP2A is cell cycle

Figure 1. Drug Screen Reveals that p53 Deficiency Is Synthetically Lethal with Topo Inhibitors

(A) DiFLC assay. Percentages of GFP ($p53^{+/+}$) or RFP ($p53^{-/-}$) cells normalized to DMSO controls. DSI values are $\log_2$ values of normalized percent GFP/normalized percent RFP ratios (Experimental Procedures). Corresponding DSI values and fold sensitivity are indicated in the color scale bar. Two concentrations of each drug (Table S2) are represented in color map; DSI values < 0 (red) and > 0 (green) indicate sensitization of p53 wild-type and p53-deficient cells, respectively. Asterisk indicates drug effects >100-fold sensitivity of RFP cells over GFP cells. conc, concentration.

(B) Drugs ranked by DSI values.

(C) Drug sensitivity validated with WST1 cell viability.

(D) HCT116 $p53^{+/+}$ (GFP-labeled) cells stably transduced with lentiviral shVector or p53-specific shRNAs shp53.3, shp53.5, and shp53.6, co-cultured with parental HCT116 $p53^{+/+}$ cells, and treated with Dox for 24 hr. Percentage of GFP-positive cells was assessed 5 days post-recovery. Three independent experiments were performed. WB validates p53 knockdown. UT, untreated.

(E) Dox-treated (for 24 hr) HCT116 and MCF10A $p53^{+/+}$ and $p53^{-/-}$ cells stained with crystal violet 12 days post-recovery. Bottom panel: Bright-field images of Dox-treated wild-type HCT116 and MEFs and derivatives carrying homozygous deletions of the p53 gene 5 days post-recovery.

(F) TOP2A, TOP2B, and TOP1 WB in HCT116 cells.

Error bars indicate SD. See also Table S2.

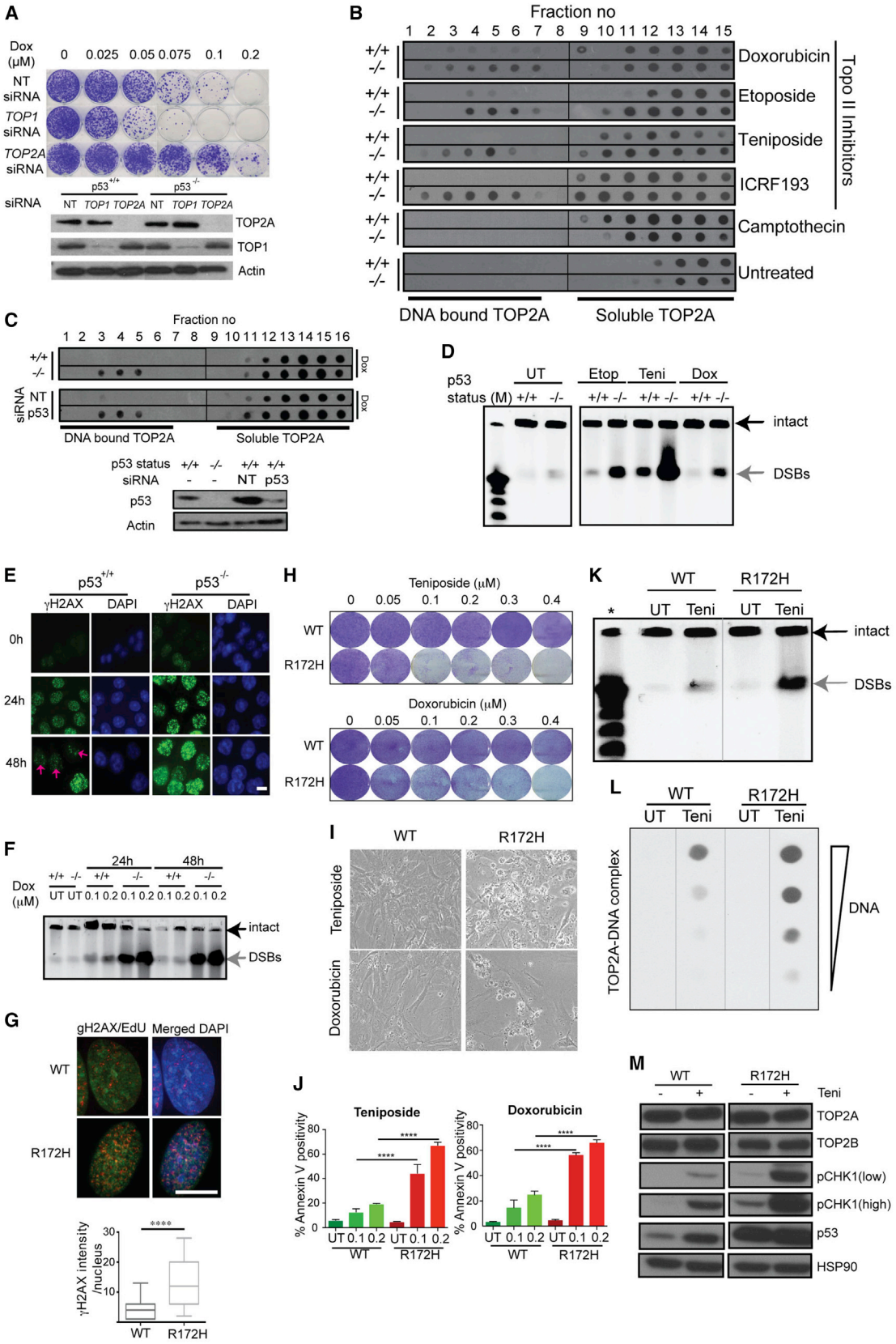

(legend on next page)

regulated and more abundant in the S- and G2/M phases (Heck et al., 1988). Notably, small interfering RNA (siRNA) to TOP2A partially rescues p53$^{-/-}$ cells in both colony survival and DiFLC assays in response to Dox, Teni, and Etop (Figure 2A; Figure S3A), confirming TOP2A as a key target for Topo II poisons (Figure 2A). In contrast, TOP2B siRNA did not rescue viability in p53$^{-/-}$ cells (Figure S3B). As expected, TOP1 siRNA sensitizes cells to the effects of Topo II inhibition by Dox (Figure 2A) (Burgess et al., 2008).

Loss of p53 Stabilizes TOP2A-DNA Complexes Causing DSBs

Topo inhibitors like Dox, Etop, and Teni act to stabilize the transient protein-DNA complex generated during Topo activity causing potentially lethal DSBs. We analyzed the accumulation of stabilized TOP2A-DNA complexes by fractionating cell extracts on CsCl gradients and detecting TOP2A protein by dot-blot (Figure 2B). Nucleic acid measurements locate DNA-containing fractions (fractions 2–7), while the TOP2A proteins free from DNA were detected in fractions 9–15. As expected, the DNA fractions in untreated controls contain low to undetectable levels of TOP2A protein (Figure 2B). Endogenous TOP2A accumulation in the DNA fractions represents stabilized TOP2A-DNA complexes, which occur, to a greater extent in HCT116 p53$^{-/-}$ cells (Figure 2B), in response to treatment with Topo II inhibitors but not with camptothecin, a known TOP1 inhibitor. We demonstrate that a catalytic inhibitor of Topo II (ICRF-193) recapitulates the effects of Topo II poisons in p53$^{-/-}$ cells (Figure 2B). Consistently, p53 knockdown using either p53-specific shRNAs in A549 (Figure S3C) or siRNAs in HCT116 (Figure 2C) cells caused an enrichment of TOP2A-DNA complexes.

Using pulsed-field gel electrophoresis (PFGE) to precisely assess DSBs induction, compared to wild-type cells, we observed extensive DSBs in HCT116 p53$^{-/-}$ cells treated with Topo II poisons and a catalytic inhibitor ICRF193 (Figures 2D and S3D), which is consistent with an increase in phosphorylated H2AX (ϒH2AX) foci in p53$^{-/-}$ cells (Figure 2E). A 24-hr time course analysis revealed that DSBs never accumulated in wild-type cells to significant levels, whereas in p53-deficient cells, extensive DSBs are detected even at earlier time points (Figure S4). To further prove that the effects of the drugs were specific to TOP2A, we generated a single-site mutation (K378Q) in TOP2A that renders the TOP2A protein catalytically inactive and able to form a stable protein-DNA complex (Figure S5A) (Hu et al., 1998). As we predicted, the overexpression of TOP2A-K378Q recapitulates the effects of Topo II poisons, resulting in a pronounced stabilization of TOP2A-DNA complexes in the absence of p53 (Figure S5).

We reproduced these results in MEFs: isogenic p53$^{-/-}$ MEFs accumulated more DSBs than wild-type MEFs upon drug treatment (Figure 2F). To question whether the increased sensitivity extends to cells containing a gain-of-function mutation in the p53 gene, we derived MEFs from a transgenic mouse model of the Li Fraumeni syndrome, which harbors a p53R172H mutation, corresponding to the p53R175H hotspot mutation in human cancers (Lang et al., 2004). Treatment of homozygous p53 mutant MEFs with Teni resulted in a far greater accumulation of γH2AX foci in replicating EdU (5-ethynyl-2-deoxyuridine)-positive cells, compared to wild-type MEFs (Figure 2G). The observed differential damage in S-phase cells translates to a dramatic loss of cell viability and accumulation of apoptotic cells in p53R172H MEFs when compared to wild-type MEFs (Figures 2H–2J). We verified that the DNA damage and DSBs formed in p53R172H MEFs (Figure 2K) resulted from a marked stabilization of TOP2A-DNA complexes. TOP2A-DNA complexes were stabilized to a far greater extent in p53R172H MEFs than in wild-type MEFs (Figure 2L). Equivalent expression of TOP2A and TOP2B proteins in wild-type and p53R172H MEFs was detected (Figure 2M). Stabilization of mutant p53 protein was observed in p53R172H MEFs, as reported previously (Goh et al., 2011; Lang et al., 2004; Olive et al., 2004). In line with our hypothesis that replication stress is significantly elevated in p53 mutant cells, phosphorylation on CHK1 (pCHK1) was strongly enriched in Teni-treated p53R172H MEFs (Figure 2M). Basal phosphorylation on CHK1 was also enriched (Figure 2M), indicating the presence of increased residual CHK1 signaling due to the mutation of p53 gene.

Figure 2. Preferential Stabilization of TOP2A-DNA Complexes in p53-Deficient Cells

(A) Crystal violet staining of Dox-treated HCT116 p53$^{-/-}$ cells transfected with non-targeting (NT) siRNA or TOP1 and TOP2A siRNAs. Bottom panel: WB validates TOP2A and TOP1 knockdown.

(B) CsCl gradient fractionation in HCT116 cells separates DNA-bound from soluble TOP2A protein. Dot-blot detects TOP2A protein.

(C) Dot-blot of HCT116 cells with p53 siRNA and NT siRNA. Bottom panel: WB validates p53 knockdown.

(D) PFGE detection of DSBs in HCT116 cells treated with 1.25 μM Etop, 0.1 μM Teni, and 0.2 μM Dox. (M) refers to Lambda Ladder PFG Marker. Broken DNA detected as single DNA band, according to previous protocol (Experimental Procedures). UT, untreated.

(E) Immunofluorescence of γH2AX in 0.1 μM Dox-treated cells. Scale bar, 10 μm. Pink arrows indicate cells with lower γH2AX intensity.

(F) PFGE of p53$^{+/+}$ and p53$^{-/-}$ MEFs. 0.1 or 0.2 μM Dox used for 24 hr or 48 hr.

(G) Immunofluorescence (IF) of γH2AX in 0.2 μM Teni-treated MEFs (wild-type [WT] or p53R172H) in the presence of EdU. γH2AX (red) in EdU-positive (green) nuclei quantified by ImageJ. Statistical analysis was performed using Mann-Whitney-Wilcoxon test. ***$p < 0.001$. Scale bar, 10 μm. Boxes indicate 25–75 percentile range. Upper bar represents 75–90 percentile range, and lower bar represents 10–25 percentile range.

(H) Teni- or Dox-treated (for 24 hr) MEFs stained with crystal violet 5 days post-recovery.

(I) Bright-field images of MEFs treated with 0.1 μM Teni or Dox 5 days post-recovery.

(J) Apoptotic cells were measured by annexin V positivity in MEFs 5 days post-recovery. Drug concentration in micromolar. ****$p < 0.0001$. Error bars indicate mean ± SD.

(K) PFGE of 0.2 μM Teni-treated MEFs. *Marker lane.

(L) Dot-blot of 0.2 μM Teni-treated MEFs. 20 μg, 10 μg, 5 μg, and 2.5 μg of DNA were used.

(M) WB of 0.2 μM Teni-treated MEFs. Low and high exposures are shown for pCHK1.

Error bars indicate SD.

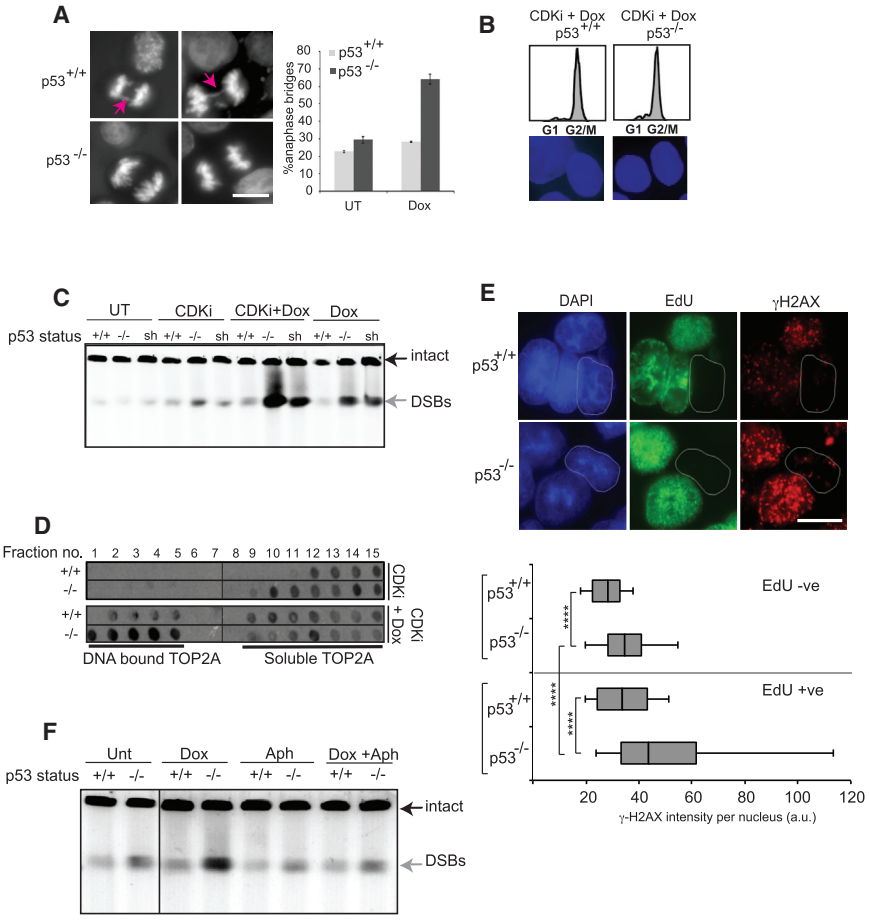

Figure 3. Topo II Inhibition Results in Replication-Associated DNA Breaks in p53-Deficient Cells

(A) Percentages of mitotic cells with anaphase bridges (pink arrows) quantified. Mean values ± SD of three independent experiments. Error bars indicate mean ± SD. Scale bar, 10 μm.

(B) FACS analysis in HCT116 cells cotreated with 9 μM CDK inhibitor RO3306 (CDKi) and 0.1 μM Dox. DAPI-stained nuclei show absence of mitotic cells.

(C) PFGE of HCT116 $p53^{+/+}$, $p53^{-/-}$, and shp53-transfected $p53^{+/+}$ cells co-treated with CDKi (9 μM) and Dox (0.1 μM). Untreated (UT), CDKi alone, and Dox alone were used as controls.

(D) Dot-blot of HCT116 cells treated with CDKi and Dox or CDKi alone.

(E) IF of γH2AX and EdU in HCT116 cells treated with EdU and 0.2 μM Teni for 3 hr. Intensity of γH2AX per nucleus was quantified by ImageJ. Statistical analysis using Mann-Whitney-Wilcoxon test. ****$p < 0.0001$. Scale bar, 10 μm. -ve, negative; +ve, positive. Gray boxes indicate 25–75 percentile range. Left bar represents 10–25 percentile range, and right bar represents 75–90 percentile range.

(F) PFGE of HCT116 $p53^{-/-}$ cells co-treated with aphidicolin and Dox or aphidicolin alone. Error bars indicate SD.

Loss of p53 Confers S-Phase-Specific DNA Damage

To distinguish whether the DNA breaks occur during failure of proper chromosome segregation in mitosis or impaired resolution of topological tensions in replication (Wang, 2002), we used a CDK1 inhibitor (RO0336), to prevent mitotic entry. Despite a significant increase in anaphase bridges in p53-deficient cells with Dox (Figure 3A), which may suggest breaks in mitosis, co-treatment with a CDK inhibitor, however, did not suppress the majority of breaks in p53-deficient cells or in cells stably expressing a p53 shRNA (Figures 3B and 3C). Furthermore, CDK inhibition did not reduce the extent of TOP2A-DNA complexes in $p53^{-/-}$ cells when co-treated with Dox (Figure 3D). These suggest that the majority of damage-induced DNA breaks and TOP2-DNA complexes in $p53^{-/-}$ cells happen during DNA replication in S phase, not from mitosis.

To determine whether such DNA damage originates from S phase, we labeled replicating cells with EdU in the presence of Teni and quantified γH2AX foci. A significant increase in γH2AX intensity was observed in the EdU-positive p53-deficient cells, suggesting S-phase damage (Figure 3E). Furthermore, aphidicolin, an inhibitor of DNA polymerase α, markedly attenuated DSBs in p53-deficient cells (Figure 3F). Together, our results clearly indicate that DNA damage in p53-deficient cells arises during replication, and the role that wild-type p53 plays in protecting against Topo II inhibition during the S phase is independent of its described G2 checkpoint function in preventing mitotic entry and chromosomal breaks (Bunz et al., 1998, 1999; Nghiem et al., 2001).

Critical Function of p53 in Maintaining Genetic Stability Is Independent of Its Canonical p21-Driven Cell-Cycle Arrest

Our results indicate that the differential DNA damage in drug-treated wild-type and p53-deficient cells is already apparent in their respective S-phase population. Furthermore, we synchronized isogenic HCT116 $p53^{+/+}$, $p53^{-/-}$, and $p21^{-/-}$ cells with hydroxyurea (HU) and analyzed TOP2A-DNA complexes after recovery in Dox (Figure 4A). Even though all cells (wild-type, $p53^{-/-}$, and $p21^{-/-}$) cycled through S phase in a synchronized manner, only $p53^{-/-}$ accumulated complexes (Figure 4B), consistent with a selective decrease in viability of $p53^{-/-}$ cells in response to Topo II inhibitors (Figure 4C). Together, our data indicate strongly that the p53-dependent response to Topo II inhibitors do not require p21. We inferred that the p21-dependent G1 checkpoint is also irrelevant to p53's function in mediating protection against Topo II inhibitors, contrary to previous reporting (Bunz et al., 1999). To further substantiate the point, we show that $p21^{-/-}$ cells are, indeed, defective in their DNA-damage-induced G1 checkpoint (Figure 4D), in response to 0.1 μM Dox, yet

proficient in preventing damage from Topo II inhibitors. In response to a lower dose of Dox (0.05 μM) that is insufficient in activating a complete cell-cycle arrest, as evidenced by the presence of bromodeoxyuridine (BrdU)-positive S-phase cells, both HCT116 $p21^{-/-}$ and $p53^{+/+}$cells show comparable cell-cycle profiles (Figures 4D and 4E), whereas a pronounced G2 checkpoint arrest is evident in $p53^{-/-}$ cells, most likely in response to unresolved damage incurred during the S phase. Western blot (WB) analysis revealed equivalent expression of TOP2A protein in HCT116 $p53^{+/+}$, $p53^{-/-}$, and $p21^{-/-}$ cells (Figure 4F). To further convince ourselves that the wild-type cells did not spontaneously arrest in G1 due to Dox, we show, using co-treatment with nocodazole to block cells in the G2/M phase, that all cells had cycled through the S phase in the same treatment period (24 hr) with Dox, resulting in only a G2/M peak (Figure S6).

Together, these data demonstrate an uncoupling between the roles of p53 in maintaining genome stability in response to Topo II inhibition and in G1 cell-cycle arrest.

Increased DNA Damage in p53-Deficient Cells Is Not Due to Defective DNA Damage and Replication Checkpoints

Topo II is thought to modulate DNA topology at sites of transcription/replication interface and to bind promoters of transcribed genes specifically in S phase (Bermejo et al., 2007, 2009). Hence, we asked whether our current observations arose from aberrant transcription/replication events. Since the replication checkpoint is important in counteracting abnormal fork transitions and disassembling the RNAP II preinitiation complex to prevent replication and transcription interference, we first analyzed whether DNA damage (DDR) checkpoints are intact in $p53^{-/-}$ cells upon Topo II inhibition. Both wild-type and p53-deficient cells display an increase in the colocalization of 53BP1 and γH2AX foci (Figure 5A), surrogate markers of the activation of the DNA DSB response, suggesting that p53 loss did not affect the initiation of early DNA damage signaling. Rather, an overall increase in 53BP1 and γH2AX foci intensity was detected in p53-deficient cells (Figure 5A). Similar kinetics of recruitment of ATR and ATM to the chromatin was observed in wild-type and p53-deficient cells (Figure 5B). Increased phospho-Chk1 and phospho-Chk2 (Figure 5B) and enhanced recruitment of other DNA damage repair proteins—namely, MRN complex (Mre11-Rad50-Nbs1) and CtIP (Figure 5C), in the p53-deficient cells—suggest that wild-type p53 plays a role in limiting DNA damage and checkpoint activation. Interestingly, we observed an intense accumulation of RNAPII (RNA polymerase II), together with TOP2A, in the $p53^{-/-}$ cells. This was also observed in p53-deficient MEFs, concomitant with the increased accumulation of Mre11, Nbs1, and Rad51 (Figure 5D). However, TOP2B protein recruitment was similar, regardless of p53 status, further proving that the genotoxicity in p53-deficient cells is specific to that of TOP2A (Figure 5D). Together, the data suggest that RNA transcription may be altered in the absence of p53, which could result in increased DNA torsional stress, generating substrates that require TOP2A activity at the chromatin to resolve.

Transcription Creates DNA Topological Conflicts in p53-Deficient Cells

To establish the involvement of transcription in increased genomic instability seen in replicating $p53^{-/-}$ cells, we inhibited RNAPII-mediated transcription using a CDK inhibitor, DRB, which blocks the elongation step of RNAPII transcription and causes premature termination (Fraser et al., 1979). We observed a significant reduction in DNA DSBs in HCT116 $p53^{-/-}$ cells co-treated with DRB and Teni, compared to Teni treatment alone (Figure 6A), which corresponded to an increased colony survival in cells similarly treated (Figure 6B), indicating that RNA transcription in the absence of p53 contributes to the genotoxicity of Teni. No marked change in cell-cycle profile was associated with DRB treatment (Figure 6C), eliminating the possibility that DRB may cause a G1 arrest and so protect cells from S-phase damage induced by Teni. Supporting the view that transcription elevates DNA supercoiling in p53-deficient cells, we show that DRB treatment greatly reduced TOP2A recruitment and TOP2A-DNA complex formation (Figure 6D), protecting $p53^{-/-}$ cells from the full toxicity of Teni. Furthermore, we show that DRB affected neither the expression of TOP2A protein nor a major replication stress-induced protein kinase, ATR, even though it clearly reduced phosphoCHK2 in p53-deficient cells (Figure 6E). Notably, DRB decreased Teni-induced pCHK2 (Figure 6E) and γH2AX (Figures 6F and 6G) predominantly in p53-deficient cells, but its effect in wild-type cells was marginal. This points to the presence of transcription-dependent damage as a major source of genomic instability in p53-deficient cells. Consistently, DRB reduces Teni-induced γH2AX foci intensity in p53-deficient cells to a level equivalent to that in Teni-treated wild-type cells. Together, our data support the model that dysregulation of replication and transcription in p53-deficient cells causes topological conflicts, explaining the increased genotoxicity toward Topo II poisons.

In accordance with our model, we predict that loss of p53 might elevate DNA replication defects. We took advantage of the DNA fiber-labeling approach, which enables replication analysis on single DNA molecules visualized by immunofluorescence (Figure 6H). DNA track lengths were measured using ImageJ. Remarkably, p53 absence impaired normal fork progression, resulting in a significant decrease in median track length from 12.05 kb (n = 110) in wild-type cells to 8.26 kb (n = 100) (Figure 6H). Significantly, transcription inhibition by DRB restores DNA track lengths in p53-deficient cells (8.32 kb; n = 100) to near wild-type levels (11.8 kb; n = 130) but has marginal effects in wild-type p53 cells, indicating that transcription impedes normal fork progression in p53-deficient cells (Figure 6I). This is consistent with our model that cells lacking p53 experience increased interference between replication and transcription, resulting in extensive fork collapse and impaired replication fork progression.

Together, our data suggest that a major source of replication stress in p53-deficient cells arises from transcription-associated damage during S phase.

In Vitro Sensitivity to Topo II Inhibitors Translates in In Vivo Tumor Xenografts

We tested the growth of HCT116 $p53^{-/-}$ spheroids in response to Dox, Etop, or Teni. Unlike wild-type cells, $p53^{-/-}$ spheroids showed more pronounced growth inhibition (Figures 7A and 7B).

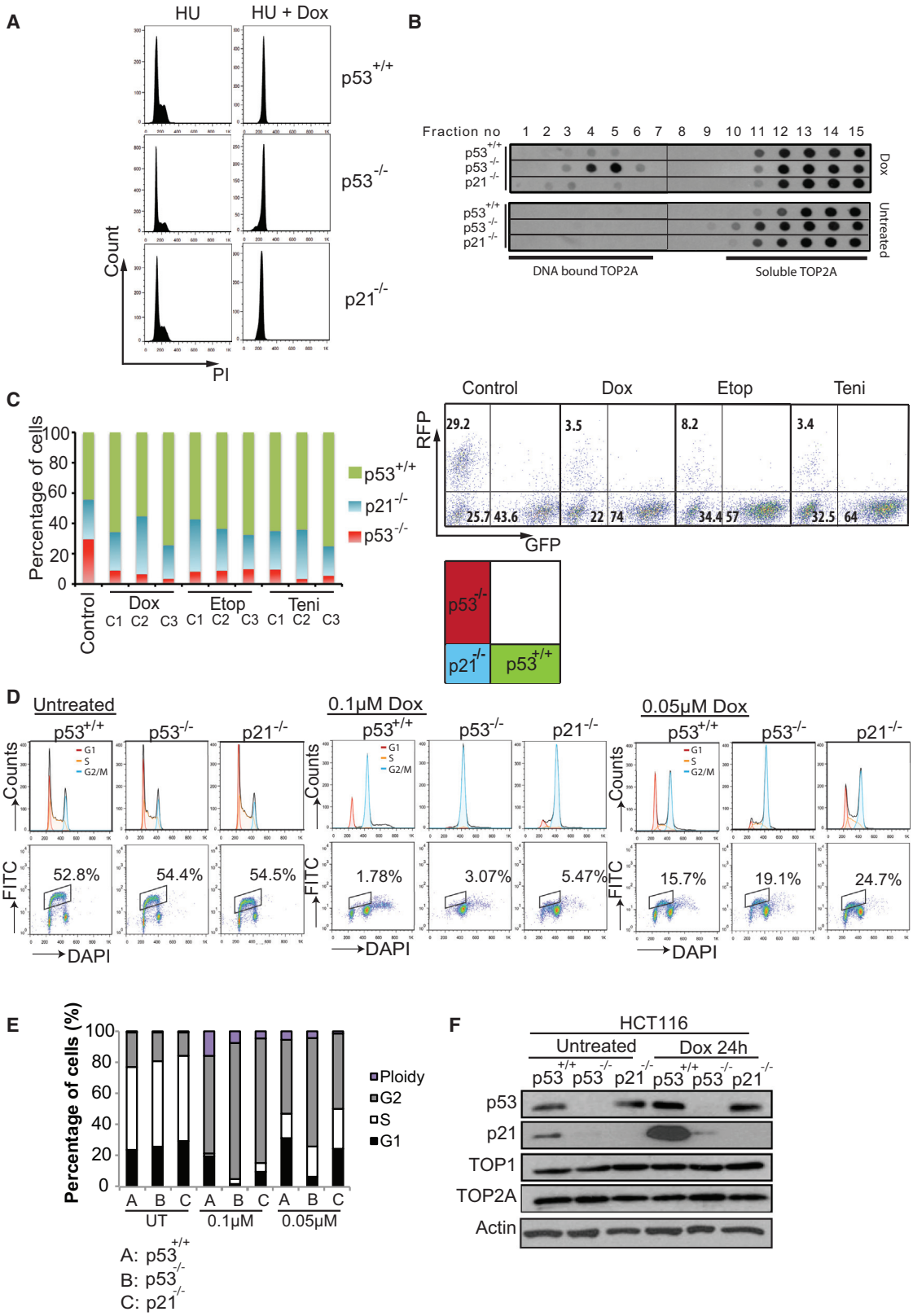

(legend on next page)

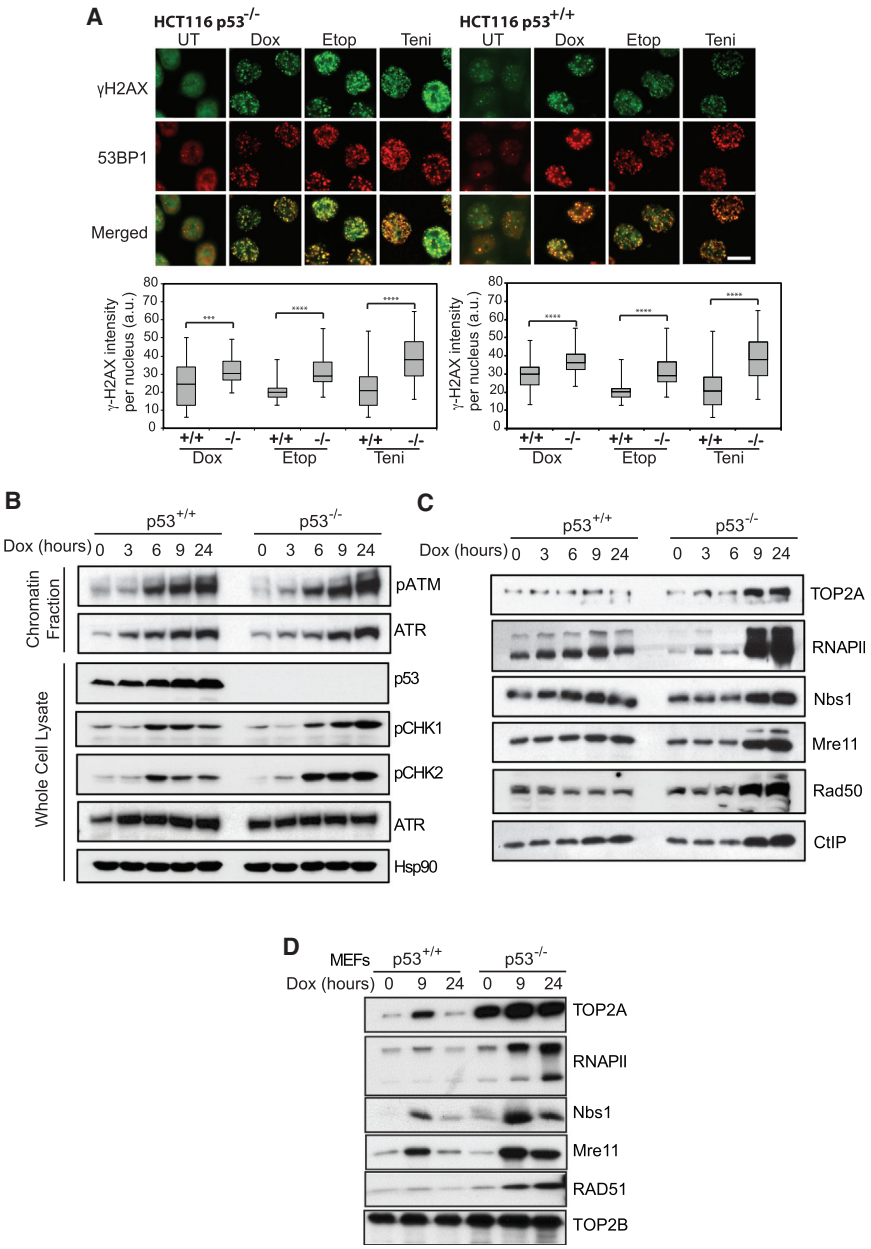

Figure 5. Intact DNA Damage Signaling and DSB Repair in the Absence of p53

(A) Colocalization of γH2AX and 53BP1 foci. Scale bar, 10 μm. Lower panel: Quantification by ImageJ. Intensity units (per nucleus) are indicated as a.u. Statistical analysis was performed using Mann-Whitney-Wilcoxon test. UT, untreated. ***$p < 0.001$; ****$p < 0.0001$. Error bars indicate SD. Boxes indicate 25–75 percentile range. Upper bar represents 75–90 percentile range, and lower bar represents 10–25 percentile range

(B) WB of chromatin fractions and whole-cell lysates in 0.1 μM Dox-treated HCT116 cells.

(C) WB of TOP2A, RNAPII, CtIP and MRN complex (Mre11-Rad50-Nbs1) in insoluble chromatin fractions (HCT116).

(D) WB of TOP2A, RNAPII, Nbs1, Mre11, RAD51, and TOP2B in insoluble chromatin fractions of 0.1 μM Dox-treated MEFs.

To understand whether these effects could extend to in vivo conditions, xenograft experiments were performed in nude mice. A significant inhibition of tumor growth was observed in Dox-treated nude mice bearing HCT116 $p53^{-/-}$ xenografts but not in untreated mice or those bearing $p53^{+/+}$ xenografts (Figure 7C). Kaplan-Meier survival analysis revealed that while all animals bearing $p53^{+/+}$ xenografts had reached endpoint (tumors > 800 mm^3) by day 50, only half of the mice in the $p53^{-/-}$ xenograft group receiving the higher drug dose reached endpoint (Figure 7D). Markedly, more cleaved caspase-3 was detected in $p53^{-/-}$ xenografts treated with Dox (Figure 7E). Similarly abundant caspase-3 activity was detected in HCT116 $p53^{-/-}$ cells, but not in HCT116 $p53^{+/+}$ cells in vitro (Figure 7F). Together, these data show that the heightened toxicity of Topo II inhibitors for $p53^{-/-}$ tumor cell lines in vitro also extends their effects in vivo in a controlled setting.

DISCUSSION

Wild-type p53 elicits a checkpoint arrest to block promiscuous S-phase entry or premature mitosis in response to ATR/CHK1 inhibition or other replication inhibitors (Nghiem et al., 2001). However, any role that p53 plays beyond its checkpoint functions in preventing

Figure 4. Wild-Type p53 Protects from Topo II Poisons through a Cell-Cycle-Arrest-Independent Function

(A) FACS (propidium iodide, PI) of HCT116 cells synchronized with 2 mM hydroxyurea (HU) and recovered in 0.1 μM Dox for 8 hr (HU + Dox). HU treatment alone (16 hr) shows cells synchronized at the G1/S phase.

(B) Dot-blot of HCT116 cells subjected to similar conditions as in (A). Untreated cells were used as controls.

(C) DiFLC assays using HCT116 $p53^{+/+}$ (GFP-labeled), HCT116 $p53^{-/-}$ (RFP-labeled), and HCT116 $p21^{-/-}$ (unlabeled) treated with three concentrations (C1, C2, and C3) of each drug. Dox: 0.05, 0.1, and 0.2 μM; Etop: 1.25, 2.5, and 5 μM; Teni: 0.05, 0.1, and 0.2 μM; Graph represents averages from at least three experiments. Right: representative FACS histograms showing percentages of each cell type in bold.

(D) FACS of HCT116 cells untreated or treated with 0.1 μM or 0.05 μM Dox. BrdU-positive population indicates S-phase cells. FITC, fluorescein isothiocyanate.

(E) Percentages of G1, S and G2/M cell population from (D) summarized in graph. UT, untreated.

(F) WB of TOP1 and TOP2A in untreated and Dox (0.1-μM)-treated HCT116 cells.

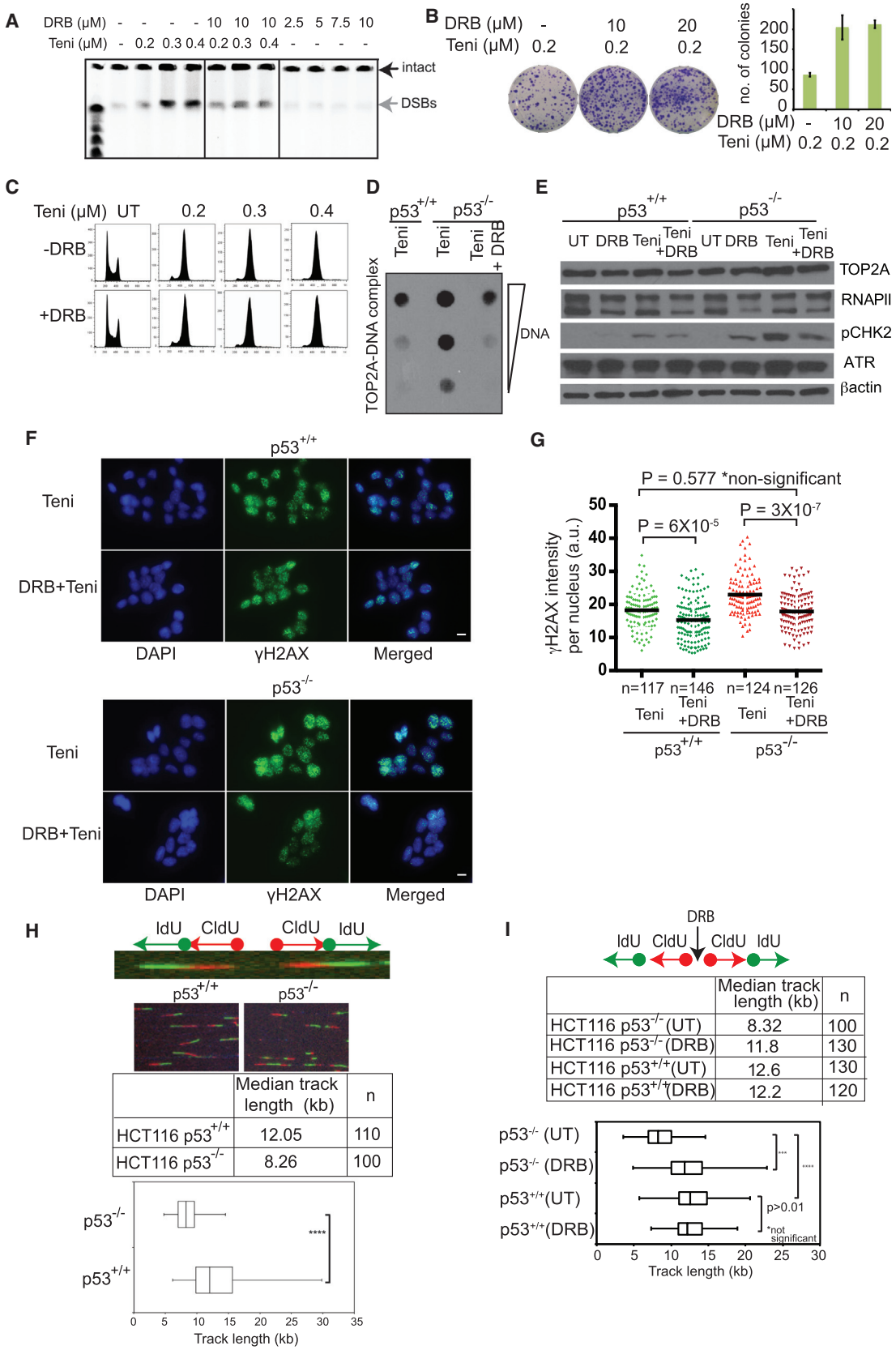

	Median track length (kb)	n
HCT116 $p53^{+/+}$	12.05	110
HCT116 $p53^{-/-}$	8.26	100

	Median track length (kb)	n
HCT116 $p53^{-/-}$ (UT)	8.32	100
HCT116 $p53^{-/-}$ (DRB)	11.8	130
HCT116 $p53^{+/+}$ (UT)	12.6	130
HCT116 $p53^{+/+}$ (DRB)	12.2	120

(legend on next page)

destabilizing replication stress is still unknown. Uncoordinated unwinding of the DNA by RNA and DNA polymerases results in topological conflicts during replication that could lead to DSBs and aberrant recombinogenic events (Azvolinsky et al., 2009; Helmrich et al., 2011). Topo II is thought to modulate DNA topology at the interface between transcription and replication (Bermejo et al., 2007, 2009). Here, in our in-depth investigations of the function of p53 in conferring "resistance" to Topo II inhibition, we used a multitude of experimental systems and isogenic cell lines to carefully dissect the checkpoint dependency and to eliminate mechanisms known to confer p53-dependent protection from DNA damage. Our data, instead, support the paradigm that p53 plays a critical role in ensuring replication integrity by preventing transcription-replication collisions and DNA topological conflicts, a role that may be critical for its function in tumor suppression.

The unexplained paradoxical observation that cells are sensitized to Dox (Bunz et al., 1999), despite the loss of p53-dependent apoptotic response, prompted us to investigate the unknown underlying mechanism. Here, we greatly extended this observation, using a systematic drug screening approach to identify common damaging lesions that may sensitize p53-deficient cells. We found that p53-deficient cells are sensitized not just to Dox but also to all Topo II poisons. Stabilization of TOP2A-DNA complexes is responsible for the observed genotoxicity in p53-deficient cells, and even in isogenic cells harboring a gain-of-function (GOF) mutation of p53 commonly found in human cancers, counter-intuitive to the expectation that GOF p53 mutation should confer resistance to DNA damage and promote cell survival (Oren and Rotter, 2010).

Although we demonstrate that the in vitro sensitivity to Topo II poisons translates into better therapeutic efficacy of p53-deficient tumor xenografts, the clinical response to Topo II poisons is a more complex integration of various other factors that may influence drug response including, for example, gain of MDR (multi-drug resistance genes) (Gottesman et al., 2002), altered homologous recombination efficiency (Treszezamsky et al., 2007), decreased repair of TOP2-DNA cleavage adducts (Cortes Ledesma et al., 2009), or altered TOP2A expression (Burgess et al., 2008). Therefore, a thorough investigation of these factors that may influence the efficacy of Topo II poisons is needed for an accurate prediction of treatment outcome. Recently, the large-scale integration of genomic data and cell-line drug sensitivity data in the Genomics of Drug Sensitivity in Cancer (GDSC) database combines cell-line drug response studies to predict biomarkers influencing drug response (Garnett and McDermott, 2012). In the GDSC database, p53 genetic status marginally influences etoposide sensitivity, with drug resistance being correlated with p53 mutation. This cautions that other factors could, indeed, modulate response to Topo II poisons, although the screening methodology (for example, assessing short-term versus longer term cell viability) could also influence the conclusions on drug-gene relationships.

Despite other known effects of Dox, we show that it acts on Topo II and causes S-phase damage in p53-deficient cells, providing us with the first set of hints that p53 renders some protective effect in S phase. By carefully dissecting the p21-dependent and p21-independent roles of p53, we found that the mechanistic role of wild-type p53 in response to Topo II inhibition is an S-phase phenomenon, not mediated through a p21-driven G1/S arrest, since $p21^{-/-}$ cells phenocopy wild-type cells (Figures 4B and 4C). Further evidence to substantiate the protective role of p53 in the S-phase is as follows: first, the differential DNA damage in wild-type and $p53^{-/-}$ cells is apparent predominantly in their S-phase population, detectable by EdU/γH2AX positivity (Figure 3E); second, DSBs that accumulated in p53-deficient cells are not a consequence of chromosomal breaks from chromosomal missegregation events during mitosis but, rather, are a result of replication processes and are attenuated by aphidicolin (Figure 3F). Third, comparison of DNA damage immediately upon completion of S phase, following a short timed-release of cells from HU-induced G1/S arrest into Dox shows that TOP2A-DNA complexes are differentially formed in wild-type and $p53^{-/-}$ cells (Figures 4A and 4B). Altogether, our data support a previously uncharacterized function of wild-type p53 in preventing topological problems and maintaining S-phase integrity.

Although many new players, including BRCA1 and DICER, have been recently reported to maintain genomic integrity by regulating replication-transcription coordination (Castel et al., 2014; Hatchi et al., 2015), a role for p53 in this context has not been described hitherto. We suggest that p53 prevents replication-transcription collisions, thereby maintaining genomic stability during DNA replication. Consistent with this, we show that pharmacologic inhibition of transcription decreases TOP2A-DNA complexes, attenuates Topo-II-poison-induced DSBs and DNA damage, and partially restores the viability of p53-deficient cells. Our results imply that, in the absence of p53, increased topological conflicts created by transcription and replication collisions create a site

Figure 6. Dysregulation of Transcription and Replication Processes May Be Alleviated by Inhibition of Transcription

(A) PFGE of HCT116 $p53^{-/-}$ cells co-treated for 24 hr with Teni and DRB. UT, Teni alone or DRB alone was used as controls.

(B) Crystal violet staining of HCT116 $p53^{-/-}$ cells treated with Teni and DRB. Teni alone was used as control. Error bars indicate mean ± SD.

(C) FACS (PI) of HCT116 $p53^{-/-}$ cells treated with Teni, with or without DRB (20 μM). UT, untreated.

(D) Dot-blot of HCT116 $p53^{-/-}$ cells co-treated with Teni (0.2 μM) and DRB (20 μM). Teni alone was used as control. 15 μg, 7.5 μg, and 3.75 μg of DNA loaded.

(E) RNAPII, TOP2A, pCHK2, ATR, and β-actin detected in whole-cell lysates.

(F) γH2AX (IF) in cells treated with 0.2 μM Teni with or without DRB for 3 hr. Scale bars, 10 μm.

(G) Distribution of γH2AX foci intensity from (F). Horizontal lines: mean values. Statistical analysis was performed using Mann-Whitney-Wilcoxon test. The p values are indicated.

(H) Single-molecule analysis of DNA replication. Insert shows a single DNA fiber labeled with 15 min chloro-deoxyuridine (CldU, red) and 15 min iodo-deoxyuridine (IdU, green). Red or green arrows indicate orientation of fork progression. DNA fiber track length quantified by ImageJ. Box represents 25–75 percentile range. Median track length and number of fiber values (n) are indicated. Statistical analysis was performed using Mann-Whitney-Wilcoxon test. ****$p < 0.0001$.

(I) Median track length in HCT116 cells pre-treated with 20 μM DRB (1 hr) quantified in graph. Statistical analysis using Mann-Whitney-Wilcoxon test. ***$p < 0.001$. Error bars indicate SD. Boxes indicate 25–75 percentile range. Left bar represents 10–25 percentile range, and right bar represents 75–90 percentile range.

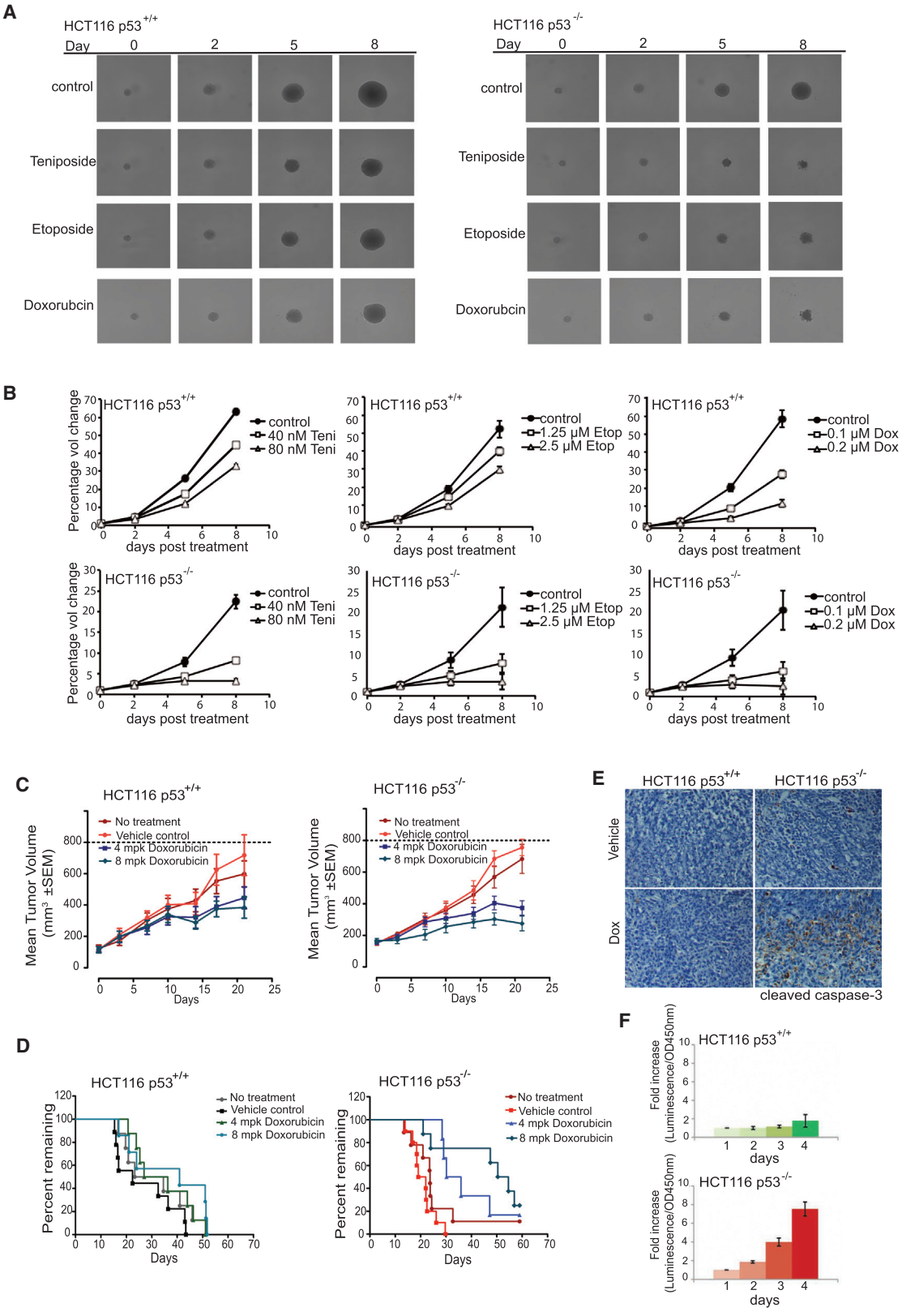

(legend on next page)

of action for TOP2A. Excessive torsional stress that accumulates may further impede replication processes.

A rational prediction of the aforementioned model is that replication defects are increased in p53-deficient cells. We found that replication fork progression is impaired in the absence of p53, even with the lack of exogenous DNA damage, suggesting that p53 acts within S phase normally to prevent DNA damage from occurring. An overall decrease in the measured DNA fiber track lengths in p53-deficient cells may occur as a result of extensive multiple replication fork collapse due to pervasive transcription interfering with replication fork progression. In line with this, transcription inhibition restores replication fork progression in p53-deficient cells and not in wild-type cells, thus providing compelling evidence that transcription contributes to chronic replication stress in the absence of wild-type p53 functions.

Our data support a paradigm shift in our understanding of p53's role in tumor suppression. We propose that an important primary function of p53, distinct from its canonical response to acute DNA damage, is to prevent the initiation of transcription-associated DNA damage and replication stress and protect against a dangerous source of endogenous DNA damage—namely, DNA replication. The pronounced selective sensitivity of p53-deficient cells specifically to Topo II poisons, and not to other DNA-damaging agents that directly cause DNA breaks, suggests that the p53-dependent response to endogenous replication stress is mechanistically different from that stimulated by acute exogenous DNA damage. Indeed, p53's response to acute DNA damage in tumor suppression has been widely debated. Acute p53 response to DNA damage was found not to contribute to p53-mediated tumor suppression in mice (Christophorou et al., 2006). Furthermore, murine models demonstrated that much of p53's transcriptional activity, as well as its functions in cell-cycle arrest and apoptosis, are dispensable for its tumor-suppressive functions (Brady et al., 2011; Li et al., 2012; Valente et al., 2013). Here, we present models to explain how p53 may guard the genome by preventing replication-dependent damage. A possibility is that p53 acts directly at the replication fork mediating fork transition and avoiding clashes with transcription complexes. Interestingly, p53 has been suggested to bind in vitro to replication forks to promote fork regression (Subramanian and Griffith, 2005), hence raising a possibility that, in cells, p53 may promote fork regression and decrease topological tensions upon any impediments to replication. Another possibility is that p53 may be required for the spatial and temporal regulation of transcription. Absence of p53 may lead to failure of proper timely regulation of transcription. In line with its reported activity in transcription repression (Murphy et al., 1999), one likely scenario in which p53 may act is to regulate transcription through reversibly suppressing transcription and avoiding unintended clashes with the replication machinery.

Our study reveals an intriguing aspect of p53-dependent response to counteract S-phase-imposed genotoxicity by preventing genetic instability arising from replication/transcription processes, thus preserving overall genomic integrity and promoting cell survival. The proposed function of p53 has far-reaching implications for its role as a tumor suppressor. We suggest that the failure to regulate conflicts between replication and transcription in cells with nonsense or missense mutations of p53 could contribute, in part, to the increased genomic instability that eventually promotes malignant transformation.

EXPERIMENTAL PROCEDURES

Co-culture Drug Screen and Calculation of the DSI

Drug titrations and WST1 cell viability assay were performed 5 days after drug recovery to establish IC_{50} (50% inhibition of growth) and LD20–LD80 (LDs resulting in 20%–80% viability) (Table S2). 1×10^4 of GFP and RFP cells were treated with various concentrations of drugs for 24 hr (or as indicated). Fluorescence-activated cell sorting (FACS) analysis (BD LSR II System BD Biosciences) was conducted to measure the percentage of GFP or RFP cells 5 days after drug recovery. Percentages of GFP cells (Y_0) and RFP cells (X_0) in DMSO-treated controls and percentages of GFP cells (Y_d) and RFP cells (X_d) in drug-treated samples were determined. The ratio of Y' ($Y' = Y_d/Y_0$) over X' ($X' = X_d/X_0$) defines the DSI ($DSI = \log_2[Y'/X']$), in which percentages of GFP or RFP cells in drug-treated samples were normalized to the DMSO controls in each experiment. Positive DSI value indicates increased drug sensitivity of HCT116 $p53^{-/-}$ (RFP) cells over HCT116 $p53^{+/+}$ (GFP) cells.

Dot-Blot Assay for Detection of TOP2A-DNA Complexes

The assay was optimized based on previously published protocols (Hartsuiker et al., 2009). Cells were lysed in 1% sarkosyl/10 mM Tris-EDTA (TE) buffer (pH 8.0), added to cesium chloride (MP Biomedicals) gradients, and ultracentrifuged at 150,000 rpm × *g* (Beckman Coulter) in a SW41 Rotor (Sorvall) at 25°C for 16 hr. Fractions were extracted, and DNA concentrations were determined using the PicoGreen assay (Life Technologies). Peak DNA-containing fractions were identified to normalize loading. The dot-blot assay was carried out in a Bio-Dot Apparatus (Bio-Rad), and samples were captured onto a 0.45-μM nitrocellulose membrane (Bio-Rad) that was blocked in 5% milk/PBST (PBS with Tween 20) before WB detection with antibodies.

PFGE

Cells were resuspended to a concentration of 10^6 cells per milliliter and mixed with an equal volume of molten 2% LMP (Low Melting Point) Agarose (Promega) before adding to plug molds (BioRad, 1703706) that were left to solidify at 4°C. Plugs were incubated in lysis buffer—100 mM EDTA [pH 8.0], 0.2% sodium deoxycholate (w/v), 1% sodium lauryl sarcosine

Figure 7. Preferential Drug Treatment Efficacy for p53-Deficient Tumors

(A) Growth of HCT116 3D spheroids monitored days after recovery from 80 nM Teni, 1.25 μM Etop, or 0.2 μM Dox.

(B) Graphic measurements of spheroids. Mean values ± SD of three to five samples. vol, volume.

(C) Tumor volume (in cubic millimeters) in mice measured after first day of drug administration (Day 0), at indicated time points. Mean tumor volume was calculated.

(D) Kaplan-Meier statistical analysis of tumor growth delay. Endpoint taken as the time required for each tumor to reach 800 mm^3.

(E) Immunohistochemistry of cryosections of tumor xenografts using cleaved caspase-3 antibody.

(F) Caspase-3 activity detected in HCT116 cells using a luminescence-based cellular assay (Caspase-Glo 3/7, Promega). Readings normalized to cell viability detected using WST1 proliferation reagent and expressed as fold increase over untreated cells. Mean values ± SD of three experiments. OD_{450}, optical density at 450 nm.

Error bars indicate mean ± SD. mpk, mg per kg.

(w/v)—at 37°C for 36–72 hr and then in washing buffer (20 mM Tris-HCL, 50 mM EDTA [pH 8.0]). Plugs were run on a 0.9% Pulsed Field Certified Agarose (BioRad, 162-0137) Tris-borate-EDTA (TBE) gel for 20 hr at 14°C, using the BioRad CHEF Mapper system. Gel running conditions were optimized to detect the migration of broken DNA as a single DNA band in gel according to previous protocol (Ray Chaudhuri et al., 2012). Gel was incubated with SYBR Gold Nucleic Acid Gel Stain (Invitrogen) and imaged using an Uvitec Cambridge imager. The marker used was Lambda Ladder PFG Marker (New England Biolabs).

SUPPLEMENTAL INFORMATION

Supplemental Information includes Supplemental Experimental Procedures, six figures, and two tables and can be found with this article online at http://dx.doi.org/10.1016/j.celrep.2016.03.011.

AUTHOR CONTRIBUTIONS

C.Y., I.A., Z.L., S.L., O.A.A., and R.K. were responsible for the experimental design and acquisition of data. K.S. and V.P. carried out the animal studies and statistical analysis of the tumor data, and V.H.B.H. performed the 3D spheroids culture experiment. C.F.C. (corresponding author) was responsible for the study conception and design and the analysis and interpretation of data. C.Y. and C.F.C. were responsible for the drafting of the manuscript.

ACKNOWLEDGMENTS

We thank Koh Han Fang for assistance with the drug screen; Prof. Marco Foiani (IFOM) and Sir David Lane (p53Lab) for scientific discussions, Dr. Massimo Lopes (University of Zurich) and Luis Coronel for technical help, and Dr. Rohit Surana for editing the manuscript. This work was supported by IFOM, the FIRC Institute of Molecular Oncology, and the A*STAR Agency for Science, Technology and Research, Singapore. We sincerely apologize to all authors whose work is not cited here due to space constraints.

Received: September 10, 2015
Revised: December 17, 2015
Accepted: February 26, 2016
Published: March 24, 2016

REFERENCES

Azvolinsky, A., Giresi, P.G., Lieb, J.D., and Zakian, V.A. (2009). Highly transcribed RNA polymerase II genes are impediments to replication fork progression in Saccharomyces cerevisiae. Mol. Cell *34*, 722–734.

Bartkova, J., Horejsí, Z., Koed, K., Krämer, A., Tort, F., Zieger, K., Guldberg, P., Sehested, M., Nesland, J.M., Lukas, C., et al. (2005). DNA damage response as a candidate anti-cancer barrier in early human tumorigenesis. Nature *434*, 864–870.

Bermejo, R., Doksani, Y., Capra, T., Katou, Y.M., Tanaka, H., Shirahige, K., and Foiani, M. (2007). Top1- and Top2-mediated topological transitions at replication forks ensure fork progression and stability and prevent DNA damage checkpoint activation. Genes Dev. *21*, 1921–1936.

Bermejo, R., Capra, T., Gonzalez-Huici, V., Fachinetti, D., Cocito, A., Natoli, G., Katou, Y., Mori, H., Kurokawa, K., Shirahige, K., and Foiani, M. (2009). Genome-organizing factors Top2 and Hmo1 prevent chromosome fragility at sites of S phase transcription. Cell *138*, 870–884.

Bester, A.C., Roniger, M., Oren, Y.S., Im, M.M., Sarni, D., Chaoat, M., Bensimon, A., Zamir, G., Shewach, D.S., and Kerem, B. (2011). Nucleotide deficiency promotes genomic instability in early stages of cancer development. Cell *145*, 435–446.

Brady, C.A., Jiang, D., Mello, S.S., Johnson, T.M., Jarvis, L.A., Kozak, M.M., Kenzelmann Broz, D., Basak, S., Park, E.J., McLaughlin, M.E., et al. (2011). Distinct p53 transcriptional programs dictate acute DNA-damage responses and tumor suppression. Cell *145*, 571–583.

Bunz, F., Dutriaux, A., Lengauer, C., Waldman, T., Zhou, S., Brown, J.P., Sedivy, J.M., Kinzler, K.W., and Vogelstein, B. (1998). Requirement for p53 and p21 to sustain G2 arrest after DNA damage. Science *282*, 1497–1501.

Bunz, F., Hwang, P.M., Torrance, C., Waldman, T., Zhang, Y., Dillehay, L., Williams, J., Lengauer, C., Kinzler, K.W., and Vogelstein, B. (1999). Disruption of p53 in human cancer cells alters the responses to therapeutic agents. J. Clin. Invest. *104*, 263–269.

Burgess, D.J., Doles, J., Zender, L., Xue, W., Ma, B., McCombie, W.R., Hannon, G.J., Lowe, S.W., and Hemann, M.T. (2008). Topoisomerase levels determine chemotherapy response in vitro and in vivo. Proc. Natl. Acad. Sci. USA *105*, 9053–9058.

Castel, S.E., Ren, J., Bhattacharjee, S., Chang, A.Y., Sánchez, M., Valbuena, A., Antequera, F., and Martienssen, R.A. (2014). Dicer promotes transcription termination at sites of replication stress to maintain genome stability. Cell *159*, 572–583.

Cheok, C.F., Verma, C.S., Baselga, J., and Lane, D.P. (2011). Translating p53 into the clinic. Nat. Rev. Clin. Oncol. *8*, 25–37.

Christophorou, M.A., Ringshausen, I., Finch, A.J., Swigart, L.B., and Evan, G.I. (2006). The pathological response to DNA damage does not contribute to p53-mediated tumour suppression. Nature *443*, 214–217.

Cortes Ledesma, F., El Khamisy, S.F., Zuma, M.C., Osborn, K., and Caldecott, K.W. (2009). A human 5′-tyrosyl DNA phosphodiesterase that repairs topoisomerase-mediated DNA damage. Nature *461*, 674–678.

Curtin, N.J. (2012). DNA repair dysregulation from cancer driver to therapeutic target. Nat. Rev. Cancer *12*, 801–817.

Di Micco, R., Fumagalli, M., Cicalese, A., Piccinin, S., Gasparini, P., Luise, C., Schurra, C., Garre', M., Nuciforo, P.G., Bensimon, A., et al. (2006). Oncogene-induced senescence is a DNA damage response triggered by DNA hyper-replication. Nature *444*, 638–642.

Dominguez-Sola, D., Ying, C.Y., Grandori, C., Ruggiero, L., Chen, B., Li, M., Galloway, D.A., Gu, W., Gautier, J., and Dalla-Favera, R. (2007). Non-transcriptional control of DNA replication by c-Myc. Nature *448*, 445–451.

Fraser, N.W., Sehgal, P.B., and Darnell, J.E., Jr. (1979). Multiple discrete sites for premature RNA chain termination late in adenovirus-2 infection: enhancement by 5,6-dichloro-1-beta-D-ribofuranosylbenzimidazole. Proc. Natl. Acad. Sci. USA *76*, 2571–2575.

Frederick, C.A., Williams, L.D., Ughetto, G., van der Marel, G.A., van Boom, J.H., Rich, A., and Wang, A.H. (1990). Structural comparison of anticancer drug-DNA complexes: adriamycin and daunomycin. Biochemistry *29*, 2538–2549.

Garnett, M.J., and McDermott, U. (2012). Exploiting genetic complexity in cancer to improve therapeutic strategies. Drug Discov. Today *17*, 188–193.

Goh, A.M., Coffill, C.R., and Lane, D.P. (2011). The role of mutant p53 in human cancer. J. Pathol. *223*, 116–126.

Gorgoulis, V.G., Vassiliou, L.V., Karakaidos, P., Zacharatos, P., Kotsinas, A., Liloglou, T., Venere, M., Ditullio, R.A., Jr., Kastrinakis, N.G., Levy, B., et al. (2005). Activation of the DNA damage checkpoint and genomic instability in human precancerous lesions. Nature *434*, 907–913.

Gottesman, M.M., Fojo, T., and Bates, S.E. (2002). Multidrug resistance in cancer: role of ATP-dependent transporters. Nat. Rev. Cancer *2*, 48–58.

Halazonetis, T.D., Gorgoulis, V.G., and Bartek, J. (2008). An oncogene-induced DNA damage model for cancer development. Science *319*, 1352–1355.

Hartsuiker, E., Neale, M.J., and Carr, A.M. (2009). Distinct requirements for the Rad32(Mre11) nuclease and Ctp1(CtIP) in the removal of covalently bound topoisomerase I and II from DNA. Mol. Cell *33*, 117–123.

Hatchi, E., Skourti-Stathaki, K., Ventz, S., Pinello, L., Yen, A., Kamieniarz-Gdula, K., Dimitrov, S., Pathania, S., McKinney, K.M., Eaton, M.L., et al. (2015). BRCA1 recruitment to transcriptional pause sites is required for R-loop-driven DNA damage repair. Mol. Cell *57*, 636–647.

Heck, M.M., Hittelman, W.N., and Earnshaw, W.C. (1988). Differential expression of DNA topoisomerases I and II during the eukaryotic cell cycle. Proc. Natl. Acad. Sci. USA *85*, 1086–1090.

Helmrich, A., Ballarino, M., and Tora, L. (2011). Collisions between replication and transcription complexes cause common fragile site instability at the longest human genes. Mol. Cell *44*, 966–977.

Hu, T., Chang, S., and Hsieh, T. (1998). Identifying Lys359 as a critical residue for the ATP-dependent reactions of Drosophila DNA topoisomerase II. J. Biol. Chem. *273*, 9586–9592.

Jackson, J.G., Pant, V., Li, Q., Chang, L.L., Quintás-Cardama, A., Garza, D., Tavana, O., Yang, P., Manshouri, T., Li, Y., et al. (2012). p53-mediated senescence impairs the apoptotic response to chemotherapy and clinical outcome in breast cancer. Cancer Cell *21*, 793–806.

Jones, R.M., Mortusewicz, O., Afzal, I., Lorvellec, M., García, P., Helleday, T., and Petermann, E. (2013). Increased replication initiation and conflicts with transcription underlie Cyclin E-induced replication stress. Oncogene *32*, 3744–3753.

Kurz, E.U., Douglas, P., and Lees-Miller, S.P. (2004). Doxorubicin activates ATM-dependent phosphorylation of multiple downstream targets in part through the generation of reactive oxygen species. J. Biol. Chem. *279*, 53272–53281.

Lang, G.A., Iwakuma, T., Suh, Y.A., Liu, G., Rao, V.A., Parant, J.M., Valentin-Vega, Y.A., Terzian, T., Caldwell, L.C., Strong, L.C., et al. (2004). Gain of function of a p53 hot spot mutation in a mouse model of Li-Fraumeni syndrome. Cell *119*, 861–872.

Li, T., Kon, N., Jiang, L., Tan, M., Ludwig, T., Zhao, Y., Baer, R., and Gu, W. (2012). Tumor suppression in the absence of p53-mediated cell-cycle arrest, apoptosis, and senescence. Cell *149*, 1269–1283.

Lord, C.J., and Ashworth, A. (2012). The DNA damage response and cancer therapy. Nature *481*, 287–294.

Lowe, S.W., Ruley, H.E., Jacks, T., and Housman, D.E. (1993). p53-dependent apoptosis modulates the cytotoxicity of anticancer agents. Cell *74*, 957–967.

Murga, M., Bunting, S., Montaña, M.F., Soria, R., Mulero, F., Cañamero, M., Lee, Y., McKinnon, P.J., Nussenzweig, A., and Fernandez-Capetillo, O. (2009). A mouse model of ATR-Seckel shows embryonic replicative stress and accelerated aging. Nat. Genet. *41*, 891–898.

Murga, M., Campaner, S., Lopez-Contreras, A.J., Toledo, L.I., Soria, R., Montaña, M.F., D'Artista, L., Schleker, T., Guerra, C., Garcia, E., et al. (2011). Exploiting oncogene-induced replicative stress for the selective killing of Myc-driven tumors. Nat. Struct. Mol. Biol. *18*, 1331–1335.

Murphy, M., Ahn, J., Walker, K.K., Hoffman, W.H., Evans, R.M., Levine, A.J., and George, D.L. (1999). Transcriptional repression by wild-type p53 utilizes histone deacetylases, mediated by interaction with mSin3a. Genes Dev. *13*, 2490–2501.

Nghiem, P., Park, P.K., Kim, Y., Vaziri, C., and Schreiber, S.L. (2001). ATR inhibition selectively sensitizes G1 checkpoint-deficient cells to lethal premature chromatin condensation. Proc. Natl. Acad. Sci. USA *98*, 9092–9097.

Olive, K.P., Tuveson, D.A., Ruhe, Z.C., Yin, B., Willis, N.A., Bronson, R.T., Crowley, D., and Jacks, T. (2004). Mutant p53 gain of function in two mouse models of Li-Fraumeni syndrome. Cell *119*, 847–860.

Oren, M., and Rotter, V. (2010). Mutant p53 gain-of-function in cancer. Cold Spring Harb. Perspect. Biol. *2*, a001107.

Ray Chaudhuri, A., Hashimoto, Y., Herrador, R., Neelsen, K.J., Fachinetti, D., Bermejo, R., Cocito, A., Costanzo, V., and Lopes, M. (2012). Topoisomerase I poisoning results in PARP-mediated replication fork reversal. Nat. Struct. Mol. Biol. *19*, 417–423.

Reaper, P.M., Griffiths, M.R., Long, J.M., Charrier, J.D., Maccormick, S., Charlton, P.A., Golec, J.M., and Pollard, J.R. (2011). Selective killing of ATM- or p53-deficient cancer cells through inhibition of ATR. Nat. Chem. Biol. *7*, 428–430.

Schoppy, D.W., Ragland, R.L., Gilad, O., Shastri, N., Peters, A.A., Murga, M., Fernandez-Capetillo, O., Diehl, J.A., and Brown, E.J. (2012). Oncogenic stress sensitizes murine cancers to hypomorphic suppression of ATR. J. Clin. Invest. *122*, 241–252.

Subramanian, D., and Griffith, J.D. (2005). p53 Monitors replication fork regression by binding to "chickenfoot" intermediates. J. Biol. Chem. *280*, 42568–42572.

Taylor, W.R., Agarwal, M.L., Agarwal, A., Stacey, D.W., and Stark, G.R. (1999). p53 inhibits entry into mitosis when DNA synthesis is blocked. Oncogene *18*, 283–295.

Toledo, L.I., Murga, M., Zur, R., Soria, R., Rodriguez, A., Martinez, S., Oyarzabal, J., Pastor, J., Bischoff, J.R., and Fernandez-Capetillo, O. (2011). A cell-based screen identifies ATR inhibitors with synthetic lethal properties for cancer-associated mutations. Nat. Struct. Mol. Biol. *18*, 721–727.

Treszezamsky, A.D., Kachnic, L.A., Feng, Z., Zhang, J., Tokadjian, C., and Powell, S.N. (2007). BRCA1- and BRCA2-deficient cells are sensitive to etoposide-induced DNA double-strand breaks via topoisomerase II. Cancer Res. *67*, 7078–7081.

Valente, L.J., Gray, D.H., Michalak, E.M., Pinon-Hofbauer, J., Egle, A., Scott, C.L., Janic, A., and Strasser, A. (2013). p53 efficiently suppresses tumor development in the complete absence of its cell-cycle inhibitory and proapoptotic effectors p21, Puma, and Noxa. Cell Rep. *3*, 1339–1345.

Vousden, K.H., and Prives, C. (2009). Blinded by the light: the growing complexity of p53. Cell *137*, 413–431.

Wang, J.C. (2002). Cellular roles of DNA topoisomerases: a molecular perspective. Nat. Rev. Mol. Cell Biol. *3*, 430–440.